ELSEVIER

Materials Science and Engineering A 438–440 (2006) 791–795

MATERIALS SCIENCE & ENGINEERING A

www.elsevier.com/locate/msea

Effects of thermo-mechanical training on a $Fe_{59}Mn_{30}Si_6Cr_5$ shape memory alloy

H.C. Lin [a,*], K.M. Lin [b], S.K. Wu [a], T.P. Wang [b], Y.C. Hsiao [b]

[a] *Department of Materials Science and Engineering, National Taiwan University, Taipei, Taiwan*
[b] *Department of Materials Science and Engineering, Feng Chia University, Taichung, Taiwan*

Received 25 April 2005; received in revised form 4 January 2006; accepted 28 February 2006

Abstract

The effects of thermo-mechanical training on a $Fe_{59}Mn_{30}Si_6Cr_5$ (numbers indicate wt.%) shape memory alloy are studied in this study. The thermo-mechanical training is carried out by controlling the training parameters of applied strain, annealing temperature and cyclic number. Experimental results show that the thermo-mechanical training can raise the stacking fault probability and reduce the critical stress of inducing ε martensite. Therefore, the ε martensite is easily stress induced from the γ matrix. The cyclic hardening phenomenon occurs at low annealing temperature due to the accumulation of Shockley partial dislocations and stacking faults introduced during the training cycles. Meanwhile, the cyclic hardening phenomenon is more significant at higher tensile strain. At higher annealing temperature, the cyclic hardening effect can be reduced by eliminating the density of the dislocations and the ε martensite can be recovered to the γ phase completely during the reverse transformation process. These features will improve the shape memory ability of $Fe_{59}Mn_{30}Si_6Cr_5$ alloy.

Keywords: FeMnSiCr shape memory alloys; Thermo-mechanical training; Stress-induced martensite

1. Introduction

In light of their low cost and excellent workability, the Fe-based shape memory alloys, which are composed of Fe–Mn–Si compositions, have attracted much attention recently. For example, the Fe–Mn–Si alloys, which contain 28–34 wt.% Mn and 4–6.5 wt.% Si, exhibit a nearly perfect shape memory effect (SME) [1–4]. The addition of Cr and Ni to the Fe–Mn–Si alloys improves their SME and corrosion resistance [5,6]. In contrast to the TiNi and Cu-based shape memory alloys, the Fe–Mn–Si alloys exhibit a non-thermoelastic martensitic transformation. Their SME arises from the reverse transformation of stress-induced ε martensite (HCP structure) into γ parent austenite (fcc structure) upon heating [1]. In the past decade, extensive studies of the Fe–Mn–Si alloys were made focusing on the transformation behavior [1,7–9], physical properties [7–10] and composition dependence of SME and corrosion resistance [5,11–14]. Also, effort is made to increase the use of these alloys, especially the "heat-to-shrink" pipe coupling [15]. More recently, the thermo-mechanical training was demonstrated to be able to improve the SME of the Fe–Mn–Si alloys [16–18]. However, the actual effects of thermo-mechanical training on these alloys have not been clarified yet. More experiments should be carried out in order to well understand this valuable technique. Therefore, in the present study, we aim to investigate systematically the effects of thermo-mechanical training on a $Fe_{59}Mn_{30}Si_6Cr_5$ shape memory alloy. Meanwhile, the effects of the training parameters of applied strain, annealing temperature and cyclic number will also be discussed.

2. Experimental procedure

A vacuum melting technique was employed to prepare the $Fe_{59}Mn_{30}Si_6Cr_5$ (wt.%) alloy. The as-cast ingot was homogenized at 1200 °C for 24 h and then hot-rolled at 1200 °C into 3-mm thickness plate. Specimens for the experiments of thermo-mechanical training were carefully cut from this as-hot-rolled plate. The experiments of thermo-mechanical training were carried out on a multi-functional tensile tester equipped with a heating furnace. During the thermo-mechanical training, the specimens were treated by the repetition of small amounts of tensile deformation ($\varepsilon = 2$–4%) at room temperature, released

* Corresponding author. Tel.: +886 2 33664532; fax: +886 2 23634562.
E-mail address: hclinntu@ntu.edu.tw (H.C. Lin).

0921-5093/$ – see front matter © 2006 Elsevier B.V. All rights reserved.
doi:10.1016/j.msea.2006.02.119

the applied stress, and then followed by a subsequent annealing at 200–600 °C for 10 min. The recording of experimental data is completely automatic; calculation and plotting points for the stress–strain curves were carried out by a digit computer. Thus the results with a rather good resolution can be obtained. X-ray diffraction (XRD) analysis was carried out at room temperature with a Philips PW1710 X-ray diffractometer under the conditions of Cu Kα radiation, 30 kV tube voltage, and 20 mA current. Specimens for transmission electron microscopy (TEM) were prepared by jet electro-polishing at −25 °C with an electrolyte consisting of 3% $HClO_4$ and 97% C_2H_5OH by volume. TEM examination was carried out by using a JEOL-1200 EX microscope at an operating voltage of 120 kV.

3. Results and discussion

Fig. 1 shows the stress–strain curves of the one to six training cycles with 3% tensile strain and 200 °C annealing for the $Fe_{59}Mn_{30}Si_6Cr_5$ alloy. In Fig. 1, the stress–strain curve of the first training cycle exhibits a steeper slope but lower flow stress than those of the subsequent training cycles. These phenomena can be explained as below. It is well known that the ε martensite can be induced from the γ austenite by the applied stress, through the formation and movement of Shockley's partial dislocations and associated stacking faults. After a critical quantity of ε martensite has been produced, the plastic deformation may come from the slip of perfect dislocations introduced in the γ austenite. Therefore, the steeper slope of stress–strain curve, which indicates a higher shear modulus, means that a higher driving force is necessary to start the formation of ε martensite by the applied stress in the first training cycle. However, the stress-induced ε martensite (or the Shockley partial dislocations and stacking faults) cannot be completely recovered to γ austenite during the following 200 °C for 10 min annealing. This suggestion is reasonable because that the finish temperature of reverse transformation from ε martensite to γ austenite for the $Fe_{59}Mn_{30}Si_6Cr_5$ alloy is even higher than 500 °C. These residual Shockley partial dislocations and stacking faults can be used as the effective nuclei to induce the ε martensite in the subsequent deformation. Namely, these effective nuclei will increase the stacking fault probability and reduce the critical stress of inducing ε martensite from the γ austenite. Therefore, the slope of stress–strain curve is smaller in the subsequent training cycles. But after the starting of stress-induced ε martensite, the further formation of ε martensite is more difficult than that occurs in the region around the nuclei. Besides, the residual Shockley's partial dislocations and stacking faults may inhibit the further formation of new Shockley partial dislocations and stacking faults. This feature will hinder the formation of stress-induced ε martensite and more perfect dislocations will occur if the applies stress is higher than a critical one. Hence, the flow stress for inducing ε martensite or perfect dislocations rises up in this stage. In Fig. 1, one can find that the flow stress increases with increasing training cycles. This behavior is similar to that as-called "cyclic hardening phenomenon". This interesting phenomenon for the $Fe_{59}Mn_{30}Si_6Cr_5$ alloy is more discussed as follows. Fig. 2 shows the flow stress (ε = 3%) as a function of training cycle for the $Fe_{59}Mn_{30}Si_6Cr_5$ alloy, which has been subjected to thermo-mechanical training with 3% tensile strain and 200–600 °C annealing. As mentioned above, the residual Shockley partial dislocations and stacking faults after 200 °C for 10 min annealing will inhibit the further formation of ε martensite and raise the critical stress for inducing ε martensite and the subsequent slip of perfect dislocations. The more the training cycles, the higher the flow stresses, and the cyclic hardening phenomenon occurs. But at higher annealing temperatures, most Shockley partial dislocations and stacking faults introduced by thermo-mechanical training will be annealed out although the effective nuclei can still exist in the γ austenite matrix. Hence, the cyclic hardening phenomenon will be less obvious at higher annealing temperatures, as shown in Fig. 2.

Fig. 3(a) and (b) shows the maximum flow stress as a function of training cycle for the $Fe_{59}Mn_{30}Si_6Cr_5$ alloy with 2–4% strain and subsequent annealing at 200 and 600 °C, respectively. As can be seen in Fig. 3(a), the maximum flow stress

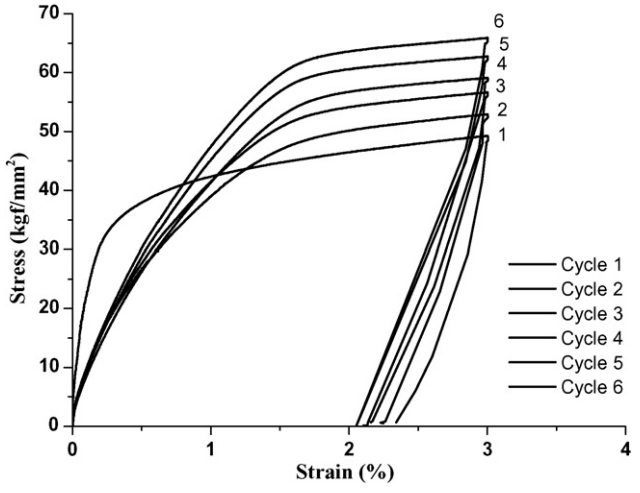

Fig. 1. The stress–strain curves of the one to six training cycles with 3% tensile strain and 200 °C annealing for the $Fe_{59}Mn_{30}Si_6Cr_5$ alloy.

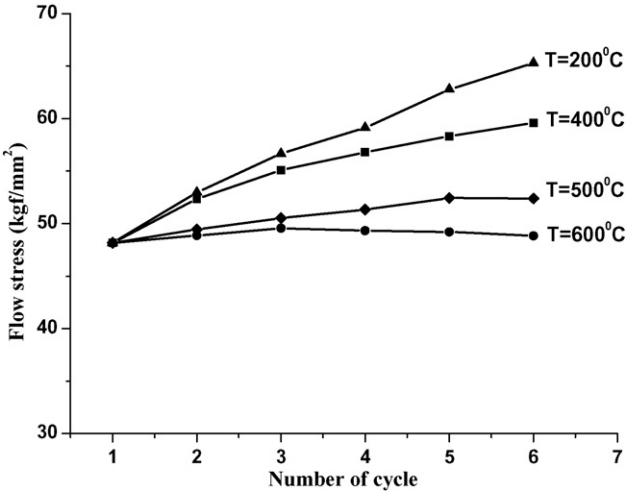

Fig. 2. The flow stress (ε = 3%) as a function of training cycle for the $Fe_{59}Mn_{30}Si_6Cr_5$ alloy, which has been subjected to thermo-mechanical training with 3% tensile strain and 200–600 °C annealing.

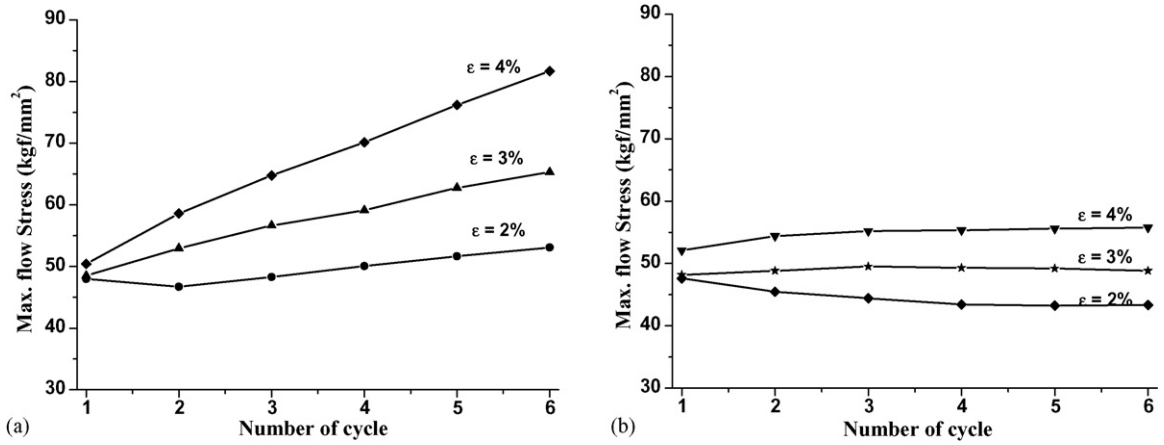

Fig. 3. The maximum flow stress as a function of training cycle for the $Fe_{59}Mn_{30}Si_6Cr_5$ alloy, which has been subjected to thermo-mechanical training with 2–4% strain and (a) 200 °C annealing, (b) 600 °C annealing.

increases with increasing training cycles at annealing temperature of 200 °C. Namely, the cyclic hardening phenomenon occurs due to the accumulation of residual Shockley partial dislocations and stacking faults because the annealing temperature is so low that these defects cannot be completely annealed out. Besides, it can also be found in Fig. 3(a) that the cyclic hardening phenomenon is more significant at higher tensile strains. In Fig. 3(b), the cyclic hardening phenomenon is not obvious for the $Fe_{59}Mn_{30}Si_6Cr_5$ alloy with 3–4% tensile strains and subsequent annealing at 600 °C. Even contrarily, there occurs the cyclic softening phenomenon for the specimens with 2% tensile strain and subsequent annealing at 600 °C. These phenomena indicate that the annealing at 600 °C can almost anneal out the introduced defects, and hence, the critical stress to induce the ε martensite is nearly the same at various training cycles. Especially for the specimens with 2% tensile strain, the effective nuclei retained in the matrix will increase the stacking fault probability and significantly reduce the critical stress of inducing ε martensite. Therefore, the maximum flow stress even decreases with increasing training cycles, as shown in Fig. 3(b).

Fig. 4 shows the shape recovery ratio as a function of training cycle for the $Fe_{59}Mn_{30}Si_6Cr_5$ alloy, which has been subjected to thermo-mechanical training with 3% tensile strain and 200–600 °C annealing. As can be seen in Fig. 4, the shape recovery ratio increases with increasing training cycles at annealing temperature of 400–600 °C, but decreases with increasing training cycles at annealing temperature of 200 °C. As mentioned above, the stress-induced ε martensite by thermo-mechanical training cannot be completely recovered to γ austenite at 200 °C for 10 min annealing. The residual ε martensite will hinder the formation of new ε martensite during the shape memory test. Hence, the shape recovery ability was depressed because the plastic deformation during the shape memory test was mainly contributed by the slip of perfect dislocations. Due to the accumulation of the irreversible ε martensite after cyclic training, the shape recovery ratio decreases with increasing training cycles, as shown in Fig. 4. However, at higher annealing temperatures of 400–600 °C, the shape recovery ratio increases with increasing training cycles. This comes from the fact that the stress-induced ε martensite by thermo-mechanical training can be almost recovered to γ austenite and the new ε martensite during the shape memory test can be easily induced by the applied stress. Besides, the retained effective nuclei of ε martensite can also promote the formation of new ε martensite. All these features will improve the specimen's shape memory ability. Hence, the shape recovery ratio can significantly increase with increasing training cycles. The shape recovery ratio can even reach 95–96% for the specimens with six training cycles and annealing at 500–600 °C.

Fig. 5 shows the XRD patterns for the $Fe_{59}Mn_{30}Si_6Cr_5$ alloy, which has been subjected to six times of thermo-mechanical training with 3% strain and annealing at 200 and 600 °C. In order to understand the existing quantities of ε martensite and γ austenite, the relative intensities of the $\varepsilon_{10\bar{1}1}$ and γ_{111} peak heights are compared. As can be seen in Fig. 5, the relative intensities of $\varepsilon_{10\bar{1}1}/\gamma_{111}$ are 0.46, 1.20 and 0.59 for the as-hot-rolled, 200 °C-annealed and 600 °C-annealed specimens, respectively. These features can be explained as below. As mentioned above, the stress-induced ε martensite by thermo-mechanical training

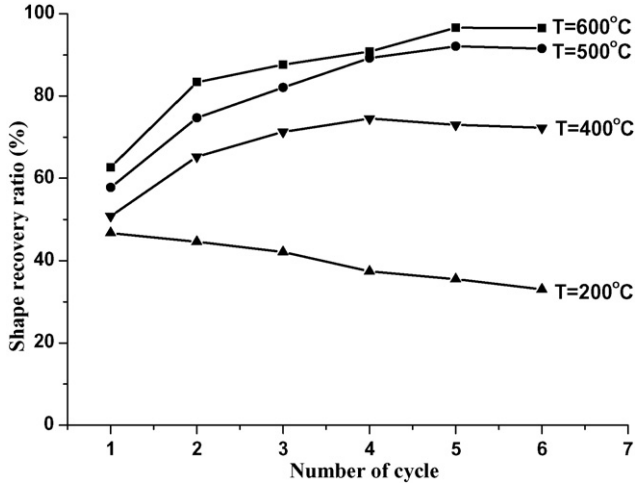

Fig. 4. The shape recovery ratio as a function of training cycle for the $Fe_{59}Mn_{30}Si_6Cr_5$ alloy, which has been subjected to thermo-mechanical training with 3% tensile strain and 200–600 °C annealing.

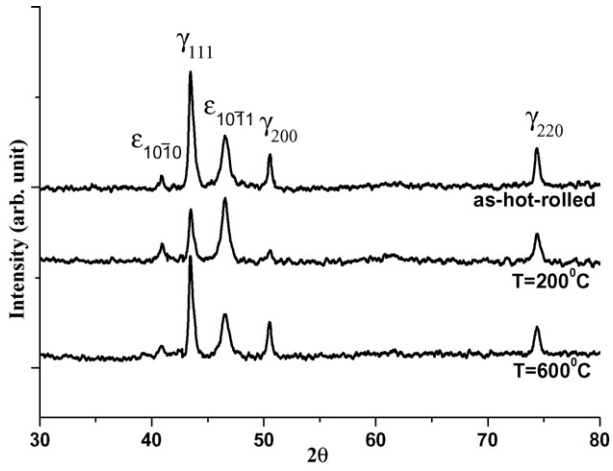

Fig. 5. The XRD patterns for the $Fe_{59}Mn_{30}Si_6Cr_5$ alloy, which has been subjected to six times of thermo-mechanical training with 3% tensile strain and annealing at 200 and 600 °C.

cannot be completely recovered to γ austenite at 200 °C for 10 min annealing. The accumulation of the irreversible ε martensite will increase the peak height of $\varepsilon_{10\bar{1}1}$ and decrease the peak height of γ_{111} after thermo-mechanical training. But for the 600 °C-annealed specimen, the stress-induced ε martensite due to thermo-mechanical training can be almost recovered to γ austenite, and hence the relative intensity of $\varepsilon_{10\bar{1}1}/\gamma_{111}$ is only slightly higher than that of the as-hot-rolled specimens after six times of training cycles.

Fig. 6(a) and (b) shows the XRD patterns for the $Fe_{59}Mn_{30}Si_6Cr_5$ alloy, which has been subjected to six times of thermo-mechanical training with 2–4% tensile strain and annealing at 200 and 600 °C, respectively. In Fig. 6(a), one can find that the value of $\varepsilon_{10\bar{1}1}/\gamma_{111}$ increases with increasing tensile strain for the 200 °C-annealed specimen. This phenomenon is reasonable because more irreversible ε martensite will retain in the matrix at higher tensile strains. Besides, the higher quantity of perfect dislocations introduced at higher tensile strains

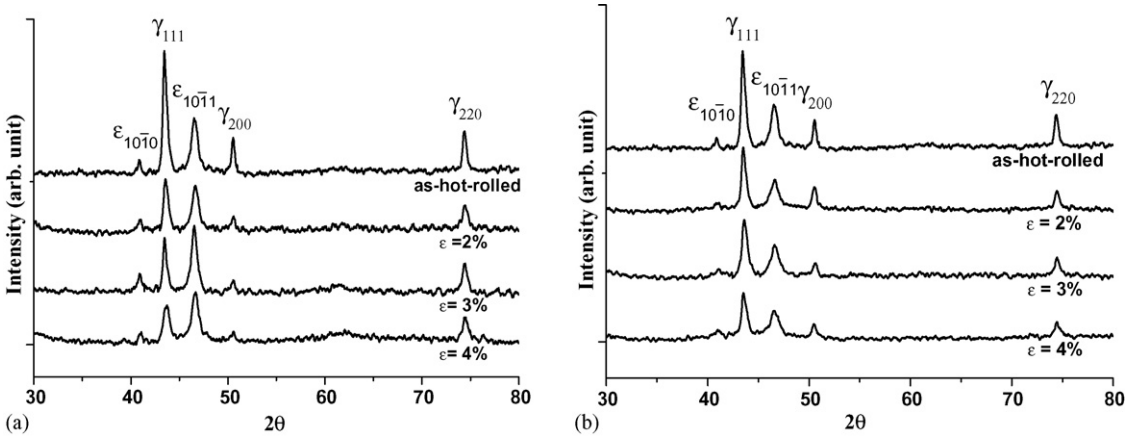

Fig. 6. XRD patterns for the $Fe_{59}Mn_{30}Si_6Cr_5$ alloy, which has been subjected to six times thermo-mechanical training with 2–4% tensile strain and (a) 200 °C annealing, (b) 600 °C annealing.

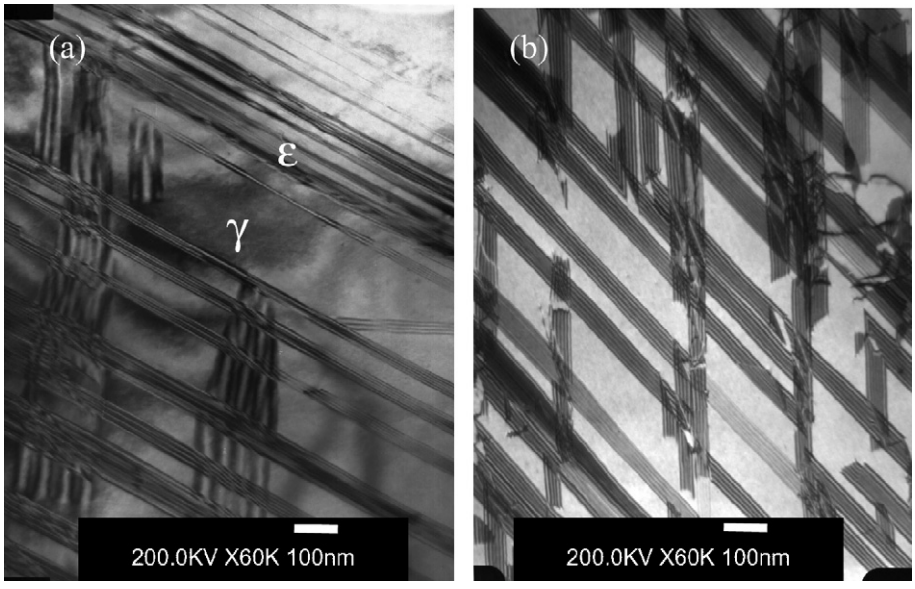

Fig. 7. TEM images of $Fe_{59}Mn_{30}Si_6Cr_5$ specimens. (a) As-hot-rolled specimen, (b) 3% strained specimen which has been subjected to six times of thermo-mechanical training with 3% tensile strain and 600 °C annealing.

will more hinder the recovery of the stress-induced ε martensite into the γ austenite, and hence the $\varepsilon_{1\,0\,\bar{1}\,1}/\gamma_{1\,1\,1}$ increases with increasing tensile strain after six times of training cycles. But for the 600 °C-annealed specimen, the stress-induced ε martensite can almost recover to the γ austenite and hence the relative intensity of $\varepsilon_{1\,0\,\bar{1}\,1}/\gamma_{1\,1\,1}$ is hardly changed although the tensile strain is increased.

Fig. 7(a) shows the TEM observation for the as-hot-rolled $Fe_{59}Mn_{30}Si_6Cr_5$ specimen. Fig. 7(b) shows the TEM observation for the 3% strained $Fe_{59}Mn_{30}Si_6Cr_5$ specimen which has been subjected to six times of thermo-mechanical training with 3% tensile strain and annealing at 600 °C. As carefully compared with Fig. 7(a) and (b), one can find that there are more homogeneous variants of ε martensite. This indicates that the thermo-mechanical training can indeed increase the stacking fault probability and promote the formation of ε martensite by tensile stress and improve their shape recovery ratio.

4. Conclusions

The effects of thermo-mechanical training on a $Fe_{59}Mn_{30}Si_6Cr_5$ shape memory alloy were investigated via the microstructural characterization, SME measurement, and tensile testing. The thermo-mechanical training can raise the stacking fault probability and reduce the critical stress of inducing ε martensite. Therefore, the ε martensite is easily stress induced from the γ matrix. The cyclic hardening phenomenon occurs at low annealing temperature due to the accumulation of Shockley's partial dislocations and stacking faults introduced during the training cycles. Meanwhile, the cyclic hardening phenomenon is more significant at higher tensile strain. At higher annealing temperature, the cyclic hardening effect can be reduced by eliminating the density of the dislocations and the ε martensite can be recovered to the γ phase completely during the reverse transformation process. These features will improve the shape memory ability of $Fe_{59}Mn_{30}Si_6Cr_5$ alloy, even up to 96% at a 3% tensile strain.

Acknowledgements

The authors are pleased to acknowledge the financial support of this research by the National Science Council (NSC), Republic of China, under Grant no. NSC 92-2216-E-035-006.

References

[1] A. Sato, E. Chishima, K. Soma, T. Mori, Acta Metall. 30 (1982) 1177.
[2] A. Sato, E. Chishima, Y. Yamaji, T. Mori, Acta Metall. 32 (1984) 539.
[3] A. Sato, K. Soma, E. Chishima, T. Mori, J. Phys. (1982) C4–C797.
[4] M. Murakami, H. Otsuka, H. Suzuki, S. Matsuda, Trans. ISIJ 27 (1987) B-88.
[5] X.X. Wang, L.C. Zhao, Scripta Metall. Mater. 26 (1992) 1451.
[6] T. Moriya, et al., Bull. JIM 29 (1990) 367 (in Japanese).
[7] H.C. Lin, K.M. Lin, Scripta Metall. Mater. 34 (1996) 343.
[8] H.C. Lin, K.M. Lin, T.S. Chou, Scripta Metall. Mater. 35 (1996) 879.
[9] M. Sade, K. Halter, E. Hornbogen, Z. Metall. 79 (1988) 487.
[10] A. Sato, Y. Yamaji, T. Mori, Acta Metall. 34 (1986) 287.
[11] T. Maki, I. Tamura, Proceedings of the ICOMAT-86 (1986) 963.
[12] M. Murakami, H. Otsuka, G. Suzuki, M. Masuda, Proceedings of the ICOMAT-86 (1986) 985.
[13] A. Sato, K. Takagaki, S. Horie, M. Kato, T. Mori, Proceedings of the ICOMAT-86 (1986) 979.
[14] O. Soderberg, X.W. Liu, P.G. Yakovenko, K. Ullakko, V.K. Lindroos, Mater. Sci. Eng. A 273–275 (1999) 543.
[15] H. Tanahashi, T. Maruyama, H. Kubo, Trans. Mater. Soc., Jpn. B 18 (1994) 1149.
[16] K. Tsuzaki, M. Ikegami, Y. Tomota, T. Maki, Trans. ISIJ 30 (1990) 666.
[17] B.H. Jiang, T. Tadaki, H. Mori, T.Y. Hsu, Mater. Trans. JIM 38 (1997) 1072–1078.
[18] B.H. Jiang, X.A. Qi, W.M. Zhou, Z.L. Xi, T.Y. Hsu, Scripta Metall. Mater. 34 (1996) 1437.